ESPL WILEY

The timing of the deglaciation in the Atlantic Iberian mountains: Insights from the stratigraphic analysis of a lake sequence in Serra da Estrela (Portugal)

Armand Hernández[1] | Alberto Sáez[2] | Ricardo N. Santos[3] |
Teresa Rodrigues[3,4] | Celia Martin-Puertas[5] | Graciela Gil-Romera[6] |
Mark Abbott[7] | Rafael Carballeira[1] | Pedro Costa[8,9] | Santiago Giralt[10] |
Sandra D. Gomes[3,11] | Melissa Griffore[7] | Jordi Ibañez-Insa[10] | Manel Leira[12] |
João Moreno[9] | Filipa Naughton[3,4] | Dulce Oliveira[4] | Pedro M. Raposeiro[13,14] |
Ricardo M. Trigo[9,15] | Gonçalo Vieira[16,17] | Alexandre M. Ramos[9,18]

[1]Centro Interdisciplinar de Química e Bioloxía (CICA), Facultade de Ciencias, GRICA group, Universidade da Coruña, A Coruña, Spain

[2]UB-Geomodels Research Institute, Universitat de Barcelona, Barcelona, Spain

[3]Portuguese Institute for Sea and Atmosphere (IPMA), Lisboa, Portugal

[4]Center of Marine Sciences (CCMAR), Algarve University, Faro, Portugal

[5]Department of Geography, Royal Holloway University of London, Egham, Surrey, UK

[6]Department of Ecology, Philipps-Marburg University, Marburg, Germany

[7]Department of Geology and Environmental Science, University of Pittsburgh, Pittsburgh, PA, USA

[8]Department of Earth Sciences, University of Coimbra, Coimbra, Portugal

[9]Instituto Dom Luiz (IDL), Faculdade de Ciências, Universidade de Lisboa, Lisbon, Portugal

[10]Geosciences Barcelona (GEO3BCN-CSIC), Barcelona, Spain

[11]School of Environment, Education and Development (SEED), The University of Manchester, Manchester, UK

[12]Centro de Investigaciones Científicas Avanzadas, Universidade da Coruña, BioCost group, A Coruña, Spain

[13]CIBIO, Centro de Investigação em Biodiversidade e Recursos Genéticos, InBIO Laboratório Associado, Pólo dos Açores, Ponta Delgada, Portugal

[14]Faculdade de Ciências e Tecnologia, Universidade dos Açores, Ponta Delgada, Portugal

[15]Departamento de Meteorologia, Universidade Federal do Rio de Janeiro, Rio de Janeiro, Brazil

[16]Centro de Estudos Geográficos, IGOT, Universidade de Lisboa, Lisbon, Portugal

[17]Laboratório Associado TERRA, Instituto Superior de Agronomia, Lisbon, Portugal

[18]Institute of Meteorology and Climate Research, Karlsruhe Institute of Technology, Karlsruhe, Germany

Correspondence

Armand Hernández, Centro Interdisciplinar de Química e Bioloxía (CICA), Facultade de Ciencias, GRICA group, Universidade da Coruña, Rúa As Carballeiras, 15071 A Coruña, Spain.
Email: armand.hernandez@udc.es

Abstract

Understanding the environmental response to the last glacial termination in regions located in transitional climate zones such as the Atlantic Iberian mountains is crucial to estimate potential changes in regions affected by current glacial melting. We present an 8.5 m-long, solid last deglaciation and Holocene chronostratigraphic record including detailed sediment analysis from Lake Peixão, a pro-glacial lake in the Serra da Estrela (Central Portugal). The age–depth model relies on a Bayesian approach that includes 16 AMS ^{14}C dates and ^{210}Pb–^{137}CS measurements, robustly dating the lake formation at 14.7 ± 0.32 cal. ka BP. This chronological reconstruction shows an average sedimentation rate of ca. 0.07 cm yr^{-1} (15 yr cm^{-1}), enabling proxy analyses at decadal timescales. The sediment sequence is composed of five lithological units:

(U1) coarse and unsorted fluvioglacial lacustrine deposits; (U2) massive fluvioglacial lacustrine deposits (863–790 cm below surface [bsf]; 14.7 ± 0.32–13.8 ± 0.12 cal. ka BP); (U3) water current fluvioglacial lacustrine deposits (790–766 cm bsf; 13.8 ± 0.12–12.9 ± 0.29 cal. ka BP); (U4) laminated/banded lacustrine deposits characterized by terrigenous deposits from ice-covered lake periods and episodic events of ice and snow melting (766–752 cm bsf; 12.9 ± 0.29–11.7 ± 0.15 cal. ka BP); and (U5) massive muddy lacustrine deposits (752–0 cm bsf; 11.7 ± 0.15 cal. ka BP–present). The occurrence of U2 to U4 deposits defines the transition from glacial cold (U1) to net warm postglacial conditions (U5). These climate transitions are marked by changes in sediments and the presence of very low sedimentation rate periods, possibly related to the Intra-Allerød Cold Period and the coldest phase of the Younger Dryas. Our results support the previously proposed timing of the retreat of the Serra da Estrela glaciers ca. 13.8 ± 0.12 cal. ka BP. The robust chronology of Lake Peixão highlights the potential of Iberian pro-glacial lakes for dating deglaciation processes and will lead to unprecedented decadal-to-centennial timescale palaeoclimate reconstructions in this region since the last glacial–interglacial transition.

KEYWORDS
climate change, geochronology, Holocene, Iberian Peninsula, lake sediments, Late Glacial, palaeoclimate

1 | INTRODUCTION

Glacial lakes are an important component of many mountain environments, and their evolution can be associated with short- and long-term climate changes, as these lakes are commonly formed in response to glacier retreats (Wilson et al., 2018). Thus, sediments from these lakes preserve valuable information that reveals past stages in glacier advance–retreat dynamics and in environmental changes. In particular, and given the current warming scenarios, it is imperative that the palaeoclimate community assesses the pace and dynamics of the last deglaciation to better evaluate environmental responses and strategies to adapt to current climate warming (IPCC, 2022). The use of different dating techniques on outcropping glacial deposits has conditioned the understanding of glacial stages in the Iberian mountains (Oliva et al., 2019, 2021). However, in regions where glacial records are scarce, such as western Iberia, sedimentological and environmental studies based on well-dated, high-resolution glacial lake records are key.

The location of the Iberian Peninsula between (i) the Atlantic Ocean and the Mediterranean Sea; (ii) the polar and subtropical air masses; and (iii) the tilting of high- and low-pressure systems makes this region particularly sensitive to environmental changes under both present and past climate conditions (Lionello, 2012). Therefore, any insight into past climate variability during transitional periods, such as the Late Quaternary glacial–interglacial period, is critical to produce well-informed climate change models. However, data to reconstruct major climatic shifts during the Late Pleistocene and the Holocene in western Iberia are still limited (e.g., López-Sáez et al., 2020; Muñoz Sobrino et al., 2013; Sánchez-López et al., 2016); in particular, there is still a lack of coherent understanding of climatic change patterns in the Iberian Central Range (ICR) during the last glacial–interglacial transition.

Extremely well-preserved glacial landforms and deposits can be found in the Serra da Estrela, a mountain range of the western and moister sector of the ICR. However, these sites are chronologically poorly defined (Vieira et al., 2021). A recent study by Vieira et al. (2021) found, by mapping and dating exposed glacial deposits, that the timing of the last deglaciation of the Serra da Estrela coincided with the onset of the Bølling–Allerød (B-A) period. This finding is supported by other studies in the ICR (e.g., García-Ruiz et al., 2016; Palacios et al., 2012). Additionally, recent regional palaeoclimate reconstructions from marine and lacustrine sediments show a rapid Late Glacial to interglacial transition between ca. 26 and 14 cal. ka BP (e.g., Ausín et al., 2020; Bartolomé et al., 2015; Fletcher et al., 2010; Jambrina-Enríquez et al., 2014; Wei et al., 2021), suggesting an abrupt temperature increase coinciding with shorter oscillations to cold conditions, including Heinrich Stadials 1 and 2 and the Younger Dryas (YD) (see Naughton et al., 2009, 2016 and references therein). Nevertheless, previous works based on lake sediments from Serra da Estrela (Connor et al., 2012; van der Knaap & van Leeuwen, 1995, 1997), which focused on detailed Holocene vegetation changes and wildfire impacts, provide little information for the Late Glacial–interglacial transition. Thus, a comprehensive chronology of the Serra da Estrela deglaciation can make a significant contribution to understanding the palaeoclimate history of this region in alignment with the current research priorities of the Estrela UNESCO Global Geopark (Vieira & Woronko, 2022).

Our study has generated a solid chronology for the Lake Peixão record, a glacial lake in Serra da Estrela, providing a precise and accurate timing of the last deglaciation of this mountain range. Sediment analysis, absolute radiometric dating methods (^{210}Pb, ^{137}Cs and ^{14}C) and the analysis of potential sedimentary hiatuses were applied to the lacustrine sediment stratigraphy, which provides a record of glacier retreat and subsequent lake formation during the Late Pleistocene. To
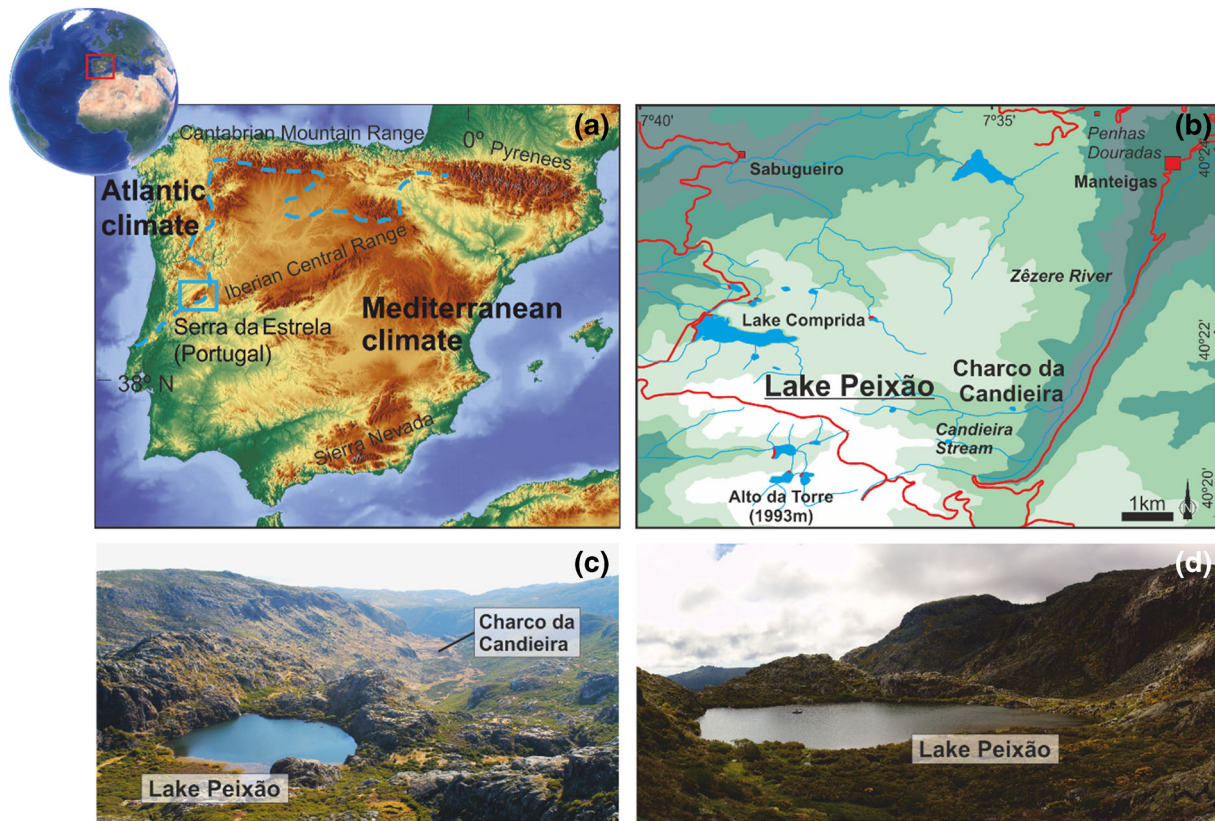
FIGURE 1 (a) Location of the study site in the Iberian Peninsula context (red box in the globe). Note that climate domains are indicated. (b) Location of the lakes Peixão, Charco da Candieira and Alto da Torre in the Serra da Estrela Natural Park. (c) Panoramic view of the glacier Candieira valley where both lakes Peixão and Charco da Candieira are located. (d) Lake Peixão photography with the Uwitec® platform indicating the position where the sediment cores were recovered. [Color figure can be viewed at wileyonlinelibrary.com]

date, Lake Peixão is the best-dated lake sediment record in Serra da Estrela from a catchment that has not been significantly altered by the construction of an artificial dam, which is common in this region. Hence, this record has the potential to provide us with an unadulterated record with multidecadal resolution to study the regional climate evolution through the Late Glacial–Holocene transition.

2 | GEOLOGICAL CONTEXT AND LAKE FEATURES

The Serra da Estrela (40°10′–40°22′N; 7°31′–7°37′W) is located in Central Portugal and has an elevation of 1993 m above sea level (asl). This granitic mountain range is the highest point in mainland Portugal (Alto da Torre). With an ENE–WSW direction cross-cutting the western Iberian Peninsula (Figure 1a), its tectonic setting generated a high relief bound by steep fault scarps on the NW and SE sides (Migoń & Vieira, 2014). This mountain range is formed by two plateaus progressively lowering towards the NE, from over 1900 to ca. 1400 m asl. The plateaus are divided by the deep Zêzere and Alforfa valleys, which follow a SSW–NNE tectonic lineament. The geological setting presents (i) Precambrian–Cambrian metasedimentary rocks (schists and greywackes); (ii) Variscan granitic rocks; and (iii) a Quaternary sedimentary cover composed of alluvial and glacial deposits.

One of the very few glacial lakes in Estrela is Lake Peixão (40°20′N; 7°36′W; 1677 m asl), which lies at the head of the

Candieira valley, 2.3 km upstream from Lake Charco da Candieira and the Zêzere glacial valley (Figure 1b). The lake has an area of 0.02 km^2, a maximum depth of ca. 5 m and a catchment area of 0.3 km^2, with a few tiny streams flowing into the lake and a small outflow (Figure 1c). Lake Peixão is oligotrophic, slightly acidic and monomictic (Boavida & Gliwicz, 1996).

3 | METHODS

Four sediment cores from Lake Peixão were retrieved in September 2015 using a UWITEC© gravity core recovery system. In addition, three other long cores were recovered in June 2019 using a UWITEC© piston coring system from a floating platform (Figure 1d). All cores were split longitudinally into two halves and imaged with a high-resolution colour line scan camera. The best-preserved gravity (PEX15-01C) and piston (PEX19-01) cores, retrieved from a similar position (less than 5 m apart) in the deepest zone of the lake (ca. 4 m depth), were chosen for analyses. PEX19-01 is an 8.63 m-long piston core overlapped by PEX15-01C (1.23 m long) in the uppermost part. Moreover, PEX19-01 has a twin core (PEX19-02) from the same position and, therefore, the same sediment composition to support the results and be employed in future studies. These cores were correlated using three 10 cm-thick sediment bands as macroscopic marker layers. All the analyses presented here, apart from the ^{210}Pb and ^{137}Cs dating performed

TABLE 1 Radiocarbon (^{14}C AMS) dates obtained from Lake Peixão. Dates over shaded bands were excluded from the age–depth model and date with * was considered inconsistent (see text)

Sample reference	Lab ID	Depth (cm)	δ^{13}C (‰)	Measured age ^{14}C (yr BP)	Median probability (cal yr BP)	2σ (cal yr AD)
PEX19-01-01-030*	UCIAMS-249101/ULA-9899	30	−27.3	1425 ± 15	1326	1300–1346
PEX19-01-01-080	UCIAMS-249102/ULA-9900	80	−26.6	1650 ± 15	1536	1516–1572
PEX19-01-01-118	UCIAMS-249103/ULA-9901	118	−27.5	2015 ± 15	1961	1922–1996
PEX19-01-01-150	UCIAMS-242267/ULA-9486	150	n/a	2545 ± 15	2717	2701–2741
PEX19-01-02-006	UCIAMS-249748/ULA-9908	181	−27.4	2325 ± 15	2346	2335–2353
PEX19-01-02-030	UCIAMS-242271/ULA-9490	205	−26.9	2360 ± 20	2356	2339–2428
PEX19-01-02-160	UCIAMS-242274/ULA-9493	335	−28.8	3670 ± 15	4029	4026–4085
PEX19-01-03-075	UCIAMS-242278/ULA-9496	435	−28.8	5490 ± 15	6293	6277–6308
PEX19-01-03-150	UCIAMS-242273/ULA-9492	510	−28.5	6110 ± 15	6977	6926–7012
PEX19-01-03-163	UCIAMS-242275/ULA-9494	523	−28.6	6345 ± 15	7267	7251–7316
PEX19-01-04-085	UCIAMS-242270/ULA-9489	627	−28.5	8330 ± 20	9358	9278–9441
PEX19-01-04-158	UCIAMS-242269/ULA-9488	703	−27.2	9590 ± 20	10 923	10 768–10 977
PEX19-01-05-015	UCIAMS-242265/ULA-9483	741	−27.6	9790 ± 20	11 218	11 193–11 242
PEX19-01-05-030	UCIAMS-242268/ULA-9487	756	−24.1	10 285 ± 20	11 989	11 929–12 101
PEX19-01-05-037	UCIAMS-242263/ULA-9481	764	−27.6	10 960 ± 20	12 862	12 810–12 910
PEX19-01-05-046	UCIAMS-242266/ULA-9484	773	−28	11 415 ± 25	13 277	13 229–13 345
PEX19-01-05-060	UCIAMS-242264/ULA-9482	788	−26.9	12 035 ± 20	13 911	13 806–14 023
PEX19-01-05-080	UCIAMS-242277/ULA-9495	809	−26.5	12 130 ± 25	14 044	13 995–14 091
PEX19-01-05-115	UCIAMS-242276/ULA-9485	845	−25.2	12 255 ± 25	14 152	14 075–14 249

on PEX15-01C, were carried out on core PEX19-01. A detailed sediment description and interpretation were performed by visual observation assisted by microscopic smear slide data obtained at every centimetre for the uppermost metre of sediments (overlapped with PEX15-01C) and at 5–10 cm resolution for the rest of the record. Mineralogical analyses were conducted by means of powder X-ray diffraction (XRD) at GEO3BCN-CSIC (Barcelona, Spain). Semi-quantitative phase analyses of the minerals in the crystalline fraction were carried out by using the Rietveld method in combination with the method of Scarlett and Madsen for the quantification of phases with partially known crystal structures using TOPAS 4.2 software from Bruker (Scarlett & Madsen, 2006). Total carbon (TC), total nitrogen (TN) (relative standard deviation, RSD = 5%), δ^{13}C and δ^{15}N (RSD = 0.05‰) analyses were conducted using a DeltaV Advantage mass spectrometer, a Conflo IV interphase and a Flash IRMS EA IsoLink CNS elemental analyser (Thermo Scientific) at Servizos de Apoio á Investigación from the Universidade da Coruña (Spain). TC and TN are expressed as percentages with respect to the total dry weight of the samples. According to the XRD results, the inorganic carbon fraction was negligible; consequently, TC was considered equal to the total organic carbon (TOC). The TOC/TN atomic ratio was calculated for all samples.

As the water–sediment interphase is best preserved in gravity cores and the compression is irrelevant in these uppermost sediments, PEX15-01C was dated by analysing ^{210}Pb in 20, 1 cm-thick intervals by alpha spectrometry and ^{214}Pb and ^{137}Cs in 14 intervals by gamma spectrometry for the upper 20 cm depth at the St. Croix Watershed Research Station, Science Museum of Minnesota (USA). The chronology for the first 20 cm was determined using the constant rate of the supply model with dating uncertainty estimated by first-order error

propagation (Appleby, 2001; Binford, 1990). The dating model was fitted to the 1963 ^{137}Cs peak. From PEX19-01, after pretreatment with acid digestion, a total of 19 samples of pollen concentrated material (Bennett & Willis, 2001) were radiocarbon dated by AMS at Laboratoire de Radiochronologie (Université de Laval, Quebec, Canada) (Table 1 and Supplementary Information). The final chronology is a Bayesian age–depth model in Bacon v. 2.5.7 (Blaauw et al., 2018) and applies the most updated Intcal20 curve for calibration of the radiocarbon dates (Reimer et al., 2020).

4 | RESULTS

4.1 | Lithological units

From master core PEX19-01, five lithological units are defined (Figure 2).

4.1.1 | Unit 1 (U1; core bottom–core catcher)

This unit represents the base of the sedimentary sequence shown in this study. Due to the resistance of the sediment infilling being drilled at 863 cm, it could not be recovered except for a few materials trapped in the core catcher, which were of different composition than the sediments deposited just above (U2). These are whitish unsorted gravelly coarse sand with angular, pebble-sized clasts, granules and no organic matter. Based on their textural characteristics and their stratigraphic context, these materials would correspond to fluvioglacial deposits that accumulated in front of the glacier.

FIGURE 2 (a) Images and stratigraphic log of the Lake Peixão sedimentary record. TOC and TOC/TN values are also shown. (b) Amplification (red rectangle) of the lowermost section of the core PEX19-01. The lithological units are indicated. Core scanner camera image of the sediments from this section are shown. Note the position of the low sedimentation periods (LSPs). See the text for further details. [Color figure can be viewed at wileyonlinelibrary.com]
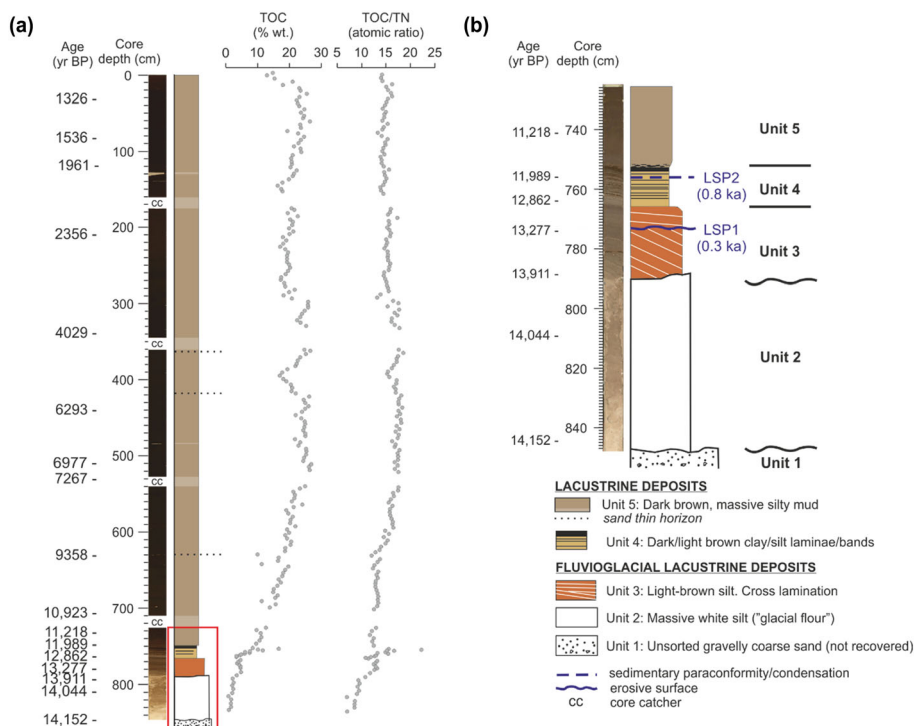
4.1.2 | Unit 2 (U2; 863–790 cm bsf)

This is a 73 cm-thick unit composed of massive, white silt and very poor in lake-origin organic remains, which are mainly made up of small *Aulacoseira* Thwaites species. Along with these, fragmented valves of benthic diatoms such as *Pinnularia viridiformis* Krammer, *Stauroneis anceps* Ehrenberg and *Pinnularia subcapitata* W. Gregory abound, but they decrease upwards. Terrestrial plant remains are also frequent. The organic matter content is the lowest of the record (TOC = 0.9–3.4% in weight [% wt.]; mean TOC = 2.2% wt.) and is mainly of lacustrine origin (TOC/TN = 7.0–10.8; mean = 9.1) (Figure 2). This unit is the richest in crystalline fraction (mean 78.4%), which is mainly composed of clay minerals. Among the other minerals, the muscovite, albite and quartz fractions are the most significant. Sediments of this unit correspond to deposits of glacial flour silty material, primarily formed by abrasion of bedrock. Once formed close to the lake, the silty materials arrived at the recently developed lake flowing by low-energy glacial meltwater stream currents. Because of the lack of stratification and current structures, these fluvioglacial deposits point to accumulation by decantation of suspended fine material that formed 'milky' plumes into the lake during fluvial flows.

4.1.3 | Unit 3 (U3; 790–766 cm bsf)

This unit is 24 cm thick and lies on an erosive surface. It is composed of light-brown silt with dispersed sand grains. Two water-current cross-lamination sets are recognized along the unit. It is poor in organic matter (TOC = 3.4–4.8% wt.; mean 4.2% wt.) (Figure 2); planktonic diatom taxa increase at the expense of benthic taxa. *Aulacoseira pfaffiana* (Reinsch) Krammer increases its relative abundance. Conversely, most benthic taxa, such as *Pinnularia microstauron* (Ehrenberg) Cleve, decrease. There are scarce terrestrial plant remains. The crystalline fraction is lower than that in U2 but is also rich in clay minerals.

The sandy nature, erosive base and water-current sedimentary structures of these sediments allow us to interpret them as fluvioglacial deposits accumulated in the lake by tractive water currents.

4.1.4 | Unit 4 (U4; 766–752 cm bsf)

This unit is 14 cm thick and displays light clayish/dark silty laminations. Light layers are 2–5 mm thick and are characterized by high contents of diatom valves (mainly *Tabellaria flocculosa* [Roth] Kützing) and clay minerals. Dark layers are 1–4 mm thick and are composed of organic matter (mainly aquatic plants, albeit terrestrial plants are also present), cladocera remains and silty detrital material. Similar laminated sediments have been seen in glacial settings (e.g., Brauer & Casanova, 2001; Turu et al., 2018), representing deposits associated with meltwater discharge which, however, were not previously described in Charco da Candieira by van der Knaap and van Leeuwen (1997). These rhythmites can have either a periodic (seasonal melting) or aperiodic (catastrophic melting events) origin. Further microscopic analysis of these sediments is needed to identify the nature of these laminations. In general, the organic matter content in U4 is higher than that in U2 and U3, with TOC values ranging between 7.6 and 16.7% wt. (mean value 10.7% wt.) and the highest values of TOC/TN = 10.8–22.2 (mean = 14.4) (Figure 2). The crystalline fraction is, however, lower than that in previous units, with a mean value of ca. 70%. This is dominated by muscovite, albite and quartz but with much lower contents of other clay minerals.

4.1.5 | Unit 5 (U5; 752–0 cm bsf)

This unit is the thickest unit of the record (752 cm thick) and is composed of dark-brown, massive mud with varying amounts of silt and dispersed sand grains. Very thin sandy horizons are present at 628, 420 and 360 cm of core depth. Sediments are rich in diatoms
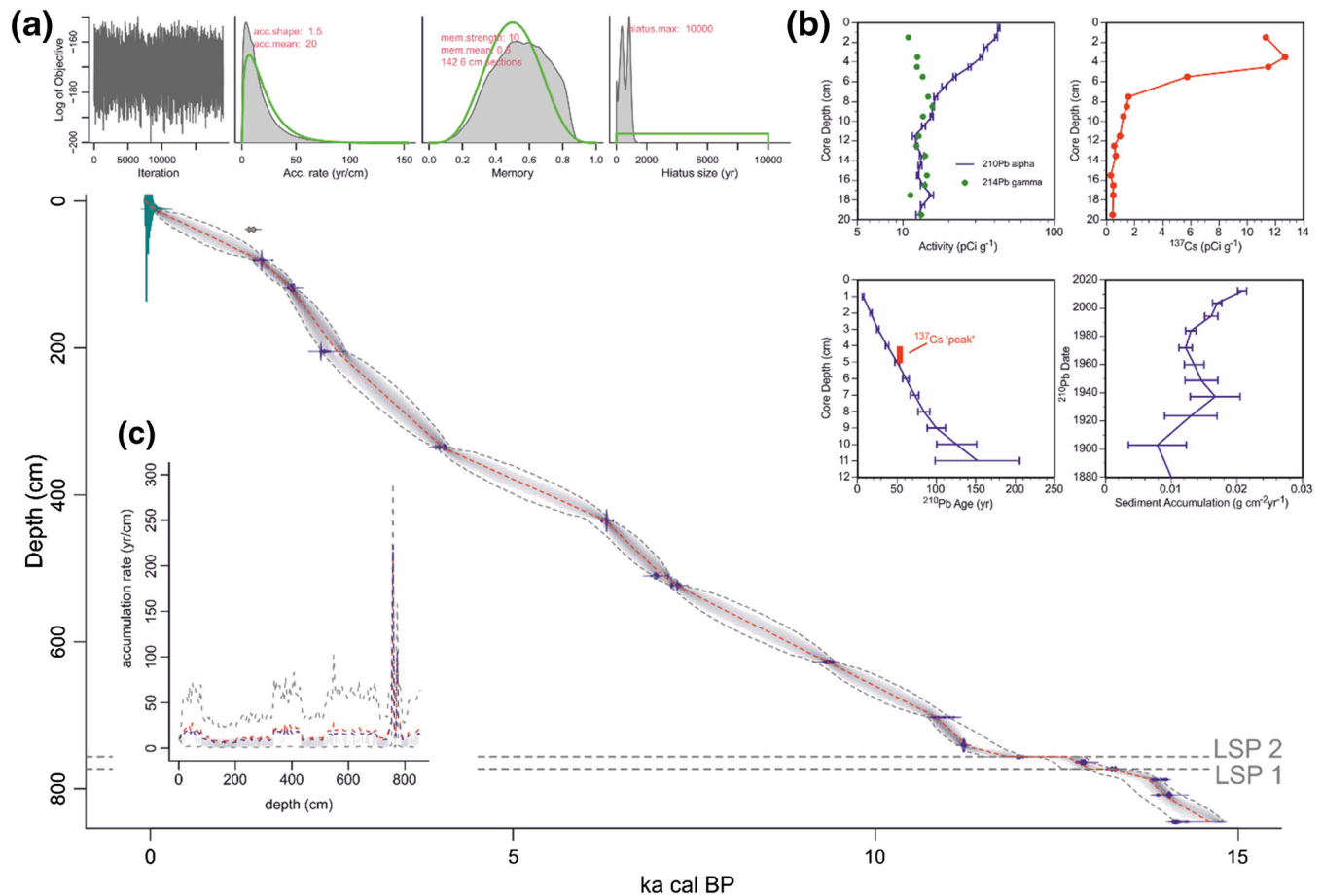
FIGURE 3 (a) Bayesian age–depth model constructed with the age–depth modelling software Bacon 2.3 (Blaauw & Christen, 2011). Dashed lines indicate the position of the gaps (see text). The uppermost four plots: (left) stability of the model; (middle-left) prior (line) and posterior (filled) distributions of accumulation mean; (middle-right) prior (line) and posterior (filled) distributions of memory properties; and (right) maximum prior (line) and actual posterior (filled) duration distribution of the hiatuses. (b) ^{210}Pb and ^{137}Cs profiles for the uppermost section of the lake sediments (see text for details). (c) Plot of the accumulation rate (yr cm^{-1}) values through the entire record for the PEXChron22 age–depth model. Dashed lines indicate median (blue), mean (red) and 95% confidence interval (grey). [Color figure can be viewed at wileyonlinelibrary.com]

and have a variable presence of cladocera, thecamoeba and chironomid remains. *Aulacoseira pfaffiana* is the dominant taxon in terms of abundance. Benthic diatom taxa are also abundant and dominated by *P. microstauron var. nonfasciata* Krammer and *Psammothidium helveticum* (Hustedt) Bukhtiyarova & Round (~10%). Other secondary diatom taxa are *Aulacoseira* sp, *P. subcapitata* and *Eunotia incisa* W. Smith ex W. Gregory. There is also particulate and amorphous organic matter, and terrestrial and aquatic plant remains such as charcoal, phytoliths and fungal spores. This unit has the highest TOC content of the record, with values from 9.7 to 27% wt. (mean = 20.7% wt.) corresponding to equivalent values of lakes from a similar context (e.g., Muñoz Sobrino et al., 2013). The TOC/TN values are lower (11.7–18.5; mean ca. 15) than in U4, indicating a more in-lake origin of the organic matter (Figure 2). Sediments of this unit correspond to shallow lacustrine deposits similar to Lake Peixão's present-day conditions, with no signs of glacier-related sedimentation.

4.2 | Age–depth modelling and sedimentary rate changes

The established age–depth model for the Peixão record (PEXChron-22) provides a robust chronology for the last ca. 14.7 cal. ka BP,

recording the formation of the lake (Figure 3). PEXChron-22 is based on 16 AMS ^{14}C dates (Table 1) and ^{137}Cs/^{210}Pb profiles (Figure 3) from the PEX19-01 and PEX15-01C cores, respectively. The chronology of the ^{210}Pb-derived interval covers the period from 2015 to 1863 CE. The ^{137}Cs profile shows the 1963 peak at 4 cm depth (12.68 pCi g^{-1}), which is used as a tie-point and drops to 0 level values below 12 cm.

The AMS ^{14}C date at 150 cm resulted in a reversal, likely due to the incorporation of removed older organic matter, whereas the sample at 180 cm was discarded for overlapping the sample at 205 cm, which is more congruent with the sedimentation rates (SRs) of U4 (Table 1; Figure 3). The radiocarbon sample at 30 cm was initially included in the age–depth model, but the MCMC iteration of the Bayesian model considered it inconsistent with the other radiocarbon dates (Table 1; Figure 3) and ^{210}Pb and ^{137}Cs measurements. Following the approaches outlined in Blaauw and Christen (2011), the prior accumulation rates for PEXChron-22 were estimated to be 20 yr cm^{-1} for the entire core to avoid perturbations in the model, whereas the accumulation shape was set to 1.5. The accumulation shape controls how much influence the accumulation rate will have on the model, and with a value of 1.5, the model has a fair amount of freedom to adapt rates to what the data suggest. The step size was set to 6 cm, which is one point more than the default for lakes, but

we obtained 142 sections, which is a fair number for a ca. 8.5 m-long record (Blaauw & Christen, 2011). Moreover, PEXChron-22 required the addition of two hiatuses or very low sedimentation periods (LSP1 = 773 cm and LSP2 = 756 cm) to produce a coherent age–depth model for the sediment description. The physical nature of these LSPs is explored in Section 5.2. The resulting age–depth model is shown in Figure 3, along with plots that describe (i) the stability of the model (log objective vs. iteration); (ii) the prior (entered by the user) and posterior (resulting) accumulation rate; and (iii) the prior and posterior memory properties.

SRs (mm yr^{-1}) were estimated based on the Bayesian model for each centimetre. Mechanical compaction due to coring, as estimated by subtracting the thickness of sediments recovered from the absolute depth drilled in each core, yielded values ranging from 1 to 7%, which have been considered for the thickness determination of the master core (PEX19-01). The SRs through the sedimentary record (Figure 3) vary between 0.1 and 1.7 mm yr^{-1} (mean 0.68 mm yr^{-1}; 15 yr cm^{-1}). The entire record covers the last 14.7 ± 0.32 cal. ka BP and the confidence interval for PEXChron-22 ranges between 4 and 317 years. The mean values of the SRs were 0.7 mm yr^{-1} (U2), 0.5 mm yr^{-1} (U3), 0.4 mm yr^{-1} (U4) and 0.8 mm yr^{-1} (U5).

5 | SIGNIFICANCE OF CHANGES IN SEDIMENTATION RATE AND RECONSTRUCTION OF THE TIMING OF THE DEGLACIATION

5.1 | Long-term evolution of Lake Peixão since the Late Glacial

Fluvial deposits forming U1–U2 and dated at 14.7 ± 0.32 cal. ka BP might indicate the initial stage of Candieira glacier retreat and the formation of the pro-glacial lake coinciding with the B-A warming (Figure 4). U3 represents fluvioglacial deposits accumulated during the second half (13.8 ± 0.12–12.9 ± 0.29 cal. ka BP) of the regionally recognized wettest period of the B-A (Naughton et al., 2016). These silty water-current fluvioglacial deposits are commonly deposited in proglacial lakes during glacier retreatment. Under these conditions, a series of melt-water channels may often have been developed during retreat as water escaping along the ice–lake contact margin during early lake formation (e.g., Fisher & Whitman, 1999). Laminations in U4 (12.9 ± 0.29–11.7 ± 0.15 cal. ka BP) correspond to sedimentation during the YD climate fluctuation (e.g., Naughton et al., 2022). These laminated/banded deposits might suggest either (i) episodes of meltwater discharge (dark layers) interrupting lake sedimentation (light layers) or (ii) sedimentation associated with a strong seasonality likely related to winter ice cover. In any case, the presence of this lamination, not described in previous works, indicates ice cover of the lake or snow accumulation in the catchment area (Figure 4) and a colder climate during the YD period than during the B-A period. U5 (11.7 ± 0.15 cal. ka BP–present) comprises the current interglacial period (i.e., the Holocene). The organic origin of the sediments indicates a clear change to shallow and mainly in-lake lacustrine muddy sediments (Figures 2 and 4b). The beginning of the deposition of these sediments and the thickness of U5 clearly indicate climate change
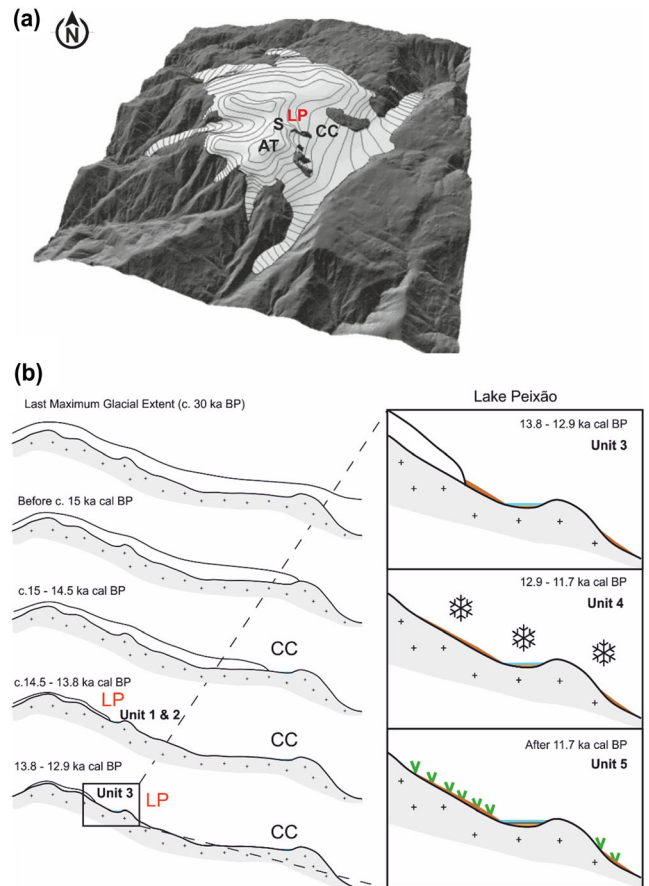

FIGURE 4 (a) Perspective of the modelled Serra da Estrela plateau icefield and valley glaciers during the maximum ice extension. View from the south, with 50 m interval contours represented over the glacier surface. Note the position of: AT, Alto da Torre (1993 m asl); S, Salgadeiras (1851 m asl); LP, Lake Peixão (1677 m asl); CC, Lake Charco da Candieira (1409 m asl). Adapted from Vieira (2008). (b) Deglaciation history of the Candieira valley during the Late Glacial–Holocene transition and the contribution of Lake Peixão. The deposition timing of each recognized sedimentary unit from the Lake Peixão record is also indicated. Note the position of Lake Peixão and Charco da Candieira. The vertical scale is magnified 2×. [Color figure can be viewed at wileyonlinelibrary.com]

after the YD towards more persistent warmer interglacial conditions (e.g., Mayewski et al., 2004).

5.2 | Low sedimentation periods significance

The LSPs (LSP1 and LSP2) detected from the chronostratigraphic analysis (i.e., detailed facies analysis and sedimentation rate evaluation) have a duration of hundreds of years, corresponding to well-known cold periods.

LSP1 from 13.2 ± 0.18 to 12.9 ± 0.21 cal. ka BP (ca. 0.3 ka) coincides with a smooth erosive surface with tilted layers below this surface and sub-horizontal or only slightly tilted layers above it (Figure 3b). This surface concurs with the Intra-Allerød Cold Period (IACP; Yu & Eicher, 2001), conditioning the drop in the SR. Moreover, despite the intra-B-A cold stage indicated for a recessional moraine in Serra de Bejar (Older Dryas, GI.1e; Carrasco et al., 2015), the absence of moraines in Serra da Estrela (Vieira, 2008; Vieira et al., 2021) points to a continuous recession of the glaciers during the B-A in the ICR

with similar altitudes (García-Ruiz et al., 2016; Palacios et al., 2012). Thus, we advocate for a cold rapid event within the warm and moist Allerød context as the most likely cause of LSP1.

LSP2 from 12.7 ± 0.07 to 11.9 ± 0.09 cal. ka BP (ca. 0.8 ka) coincides with the coldest part of the YD cold event (U4; Naughton et al., 2019, 2022). These cold conditions led to a longer duration of ice and snow cover in the lake and its catchment, leading to a decrease in high-energy runoff episodes. This provoked very low or no deposition conditions due to the absence of terrigenous inputs and diminished lake productivity, resulting in a paraconformity (Figure 2). Elsewhere in the ICR (e.g., Sierras de Gredos and Bejar), during the YD, glacier remnants, snow patches and glacial cirques were present (Carrasco et al., 2015; Oliva et al., 2019; Palacios et al., 2012), which would indicate colder regional conditions supporting our interpretation of LSP2 during the deposition of U4.

5.3 | Deglaciation timing in the western Iberian mountains

The total disappearance of glaciers in Serra da Estrela was dated using [36]Cl at approximately 14.2 ± 1.5 cal. ka BP at 1851 m asl (Vieira et al., 2021); however, and despite the consensus of a rapid deglaciation due to a sudden increase in the temperatures during the first half of the B-A period (e.g., López-Sáez et al., 2020), and assuming the errors of the dated moraines, the glacier retreat seems to have begun earlier in lower valleys (U1, Figure 4). Lake Charco da Candieira, which is 1410 m asl (Figure 1), began to accumulate organic sediments at approximately 14.8 cal. ka BP (Figure 4; van der Knaap & van Leeuwen, 1997), whereas Lake Peixao (1677 m asl) fluvioglacial sediments (U2) began their deposition at 14.7 ± 0.32 cal. ka BP (Figure 4).

The second half of the B-A period (U3) was previously considered a warmer and moister period in Serra da Estrela (van der Knaap & van Leeuwen, 1997), but higher resolution studies in the ICR have identified a rapid cooling event (IACP; López-Sáez et al., 2020; Muñoz Sobrino et al., 2013; Turu et al., 2021) during this second half of the B-A, likely responsible for LSP1 (Section 5.2). This cold period has already been identified and defined in other regional palaeoclimate studies in western Iberia. Muñoz Sobrino et al. (2013), based on chironomid and pollen analyses, defined the La Roya II cold period in agreement with Greenland Interstadial 1b (Rasmussen et al., 2006). Moreover, a recent study based on sediments from the Navamuño depression in the Sierra de Béjar (ICR) documents this cold (and dry) interval between 13.1 and 12.9 cal. ka BP (Turu et al., 2021). Nevertheless, the older study from the nearby lake Charco da Candieira (van der Knaap & van Leeuwen, 1997), based only on pollen analysis, suggested a warmer and moister climate during the Allerød (14–12.8 cal. ka BP).

The YD period has commonly been divided into different phases between 12.9 and 11.7 cal. ka BP (e.g., Bartolomé et al., 2015; Rasmussen et al., 2006). In the ICR in general and in Serra da Estrela in particular, two main YD phases have been identified (López-Sáez et al., 2020; van der Knaap & van Leeuwen, 1997). The first phase (12.9–12.4 cal. ka BP) was characterized by a warm but progressively colder and wetter climate (van der Knaap & van Leeuwen, 1997) and the coldest period after 12.4 cal. ka BP, which would have caused LSP2 in Lake Peixão. Thus, the YD includes the identified LSP2

(Section 5.2) during deposition of the laminated/banded sediments of U4, which would represent cold and likely wet climate conditions.

Finally, the current interglacial period (i.e., the Holocene; last 11.7 ka) denotes a clear rapid change to persistent warmer climates. Previous studies (e.g., Connor et al., 2012; van der Knaap & van Leeuwen, 1995, 1997) have given a broad overview of the Holocene environmental and climate evolution in Serra da Estrela divided into five major periods focused on climate and human impacts on vegetation and wildfires. These authors defined a warm and dry Early Holocene and a moister mid-Holocene with strong human impact masking climate changes after 5.7 ka BP. In addition, Connor et al. (2012) provided no clear signal of Holocene aridity, possibly because Serra da Estrela rarely experiences an intense summer drought, as is otherwise usual in Mediterranean environments. Despite these reconstructions, there is a lack of highly resolved palaeoclimate findings on local and regional settings that we propose to solve with a multiproxy analysis of Lake Peixão sediments in the future.

6 | SUMMARY AND CONCLUSIONS

The results from Lake Peixão sediments confirm and further constrain the timing of glacier retreat in the Serra da Estrela (western ICR) and landscape changes proposed by previous authors (van der Knaap & van Leeuwen, 1997; Vieira et al., 2021). The establishment of a reliable chronology based on radiometric ^{210}Pb, ^{137}Cs and ^{14}C techniques applied to lake sediments marks the formation of Lake Peixão as the result of Candieira glacier retreat. Lake Peixão was formed at ca. 14.7 cal. ka BP and was subject to fluvioglacial dynamics until 13.8 cal. ka BP. Glacier retreat from the Candieira valley led to fluvioglacial sedimentation in a recently formed lake, where only the highest points retained permanent snow patches (13.8–12.9 cal. ka BP). During this retreat, Lake Peixão recorded two episodes of severe climate conditions lasting 0.3 and 0.8 ka and corresponding to the IACP (ca. 13 ka BP) and the coldest phase of the YD (ca. 12.4 ka BP), respectively. Our results show that the latter (YD period) can be divided into two different phases, a warm to cold and wet phase between 12.9 and 12.4 cal. ka BP and a very cold phase after 12.4 cal. ka BP. The end of these long periods with snow presence in the mountains and ice-covered lakes, as a consequence of warmer postglacial conditions, occurred at 11.7 ± 0.15 cal. ka BP.

Our results showed that stratigraphic analysis in well-dated lake records is key to reconstructing different glacial stages, complementing other commonly used techniques (e.g., cosmic ray exposure dating). Moreover, the well-dated and highly resolved Lake Peixão record will enable the first decadal-to-centennial climate reconstruction of environmental and surface processes through the last 15 ka. Although detailed analyses of the record for different proxies are needed to reconstruct the decadal-to-centennial climate changes, this unique record from western Iberia influenced by the Atlantic climate will enable comparisons to other records, stimulating new investigations.

AUTHOR CONTRIBUTIONS

Armand Hernández: conceptualization; funding acquisition; methodology; investigation; supervision; writing – initial draft; writing – reviewing and editing. **Alberto Sáez:** conceptualization; methodology; investigation; supervision; writing – reviewing and editing. **Ricardo N. Santos:** conceptualization; methodology; investigation; writing – reviewing and editing. **Teresa Rodrigues:** methodology; investigation; writing – reviewing and editing. **Celia Martin-Puertas**: conceptualization; supervision; writing – reviewing and editing. **Graciela Gil-Romera:** conceptualization; methodology; supervision; writing – reviewing and editing. **Mark Abbott:** investigation; writing – reviewing and editing. **Rafael Carballeira:** writing – reviewing and editing. **Pedro Costa:** investigation; writing – reviewing and editing. **Santiago Giralt:** investigation; supervision; writing – reviewing and editing. **Sandra D. Gomes:** methodology; investigation; writing – reviewing and editing. **Melissa Griffore:** investigation; writing – reviewing and editing. **Jordi Ibañez-Insa:** investigation; writing – reviewing and editing. **Manel Leira:** writing – reviewing and editing. **João Moreno:** writing – reviewing and editing. **Filipa Naughton:** writing – reviewing and editing. **Dulce Oliveira:** writing – reviewing and editing. **Pedro M. Raposeiro:** investigation; writing – reviewing and editing. **Ricardo M. Trigo:** funding acquisition; investigation; writing – reviewing and editing. **Gonçalo Vieira:** investigation; supervision; writing – reviewing and editing. **Alexandre M. Ramos:** funding acquisition; investigation; writing – reviewing and editing.

DATA AVAILABILITY STATEMENT

Data are available as supplementary online information.

ORCID

Armand Hernández https://orcid.org/0000-0001-7245-9863
Ricardo N. Santos https://orcid.org/0000-0002-8252-3619

REFERENCES

Appleby, P.G. (2001) Chronostratigraphic techniques in recent sediments. In: Smol, J.P., Birks, H.J.B., Last, W.M., Bradley, R.S. & Alverson, K. (Eds.) *Tracking Environmental Change Using Lake Sediments: Basin Analysis, Coring, and Chronological Techniques, Developments in Paleoenvironmental Research*. Dordrecht: Springer, pp. 171–203. https://doi.org/10.1007/0-306-47669-X_9

Ausín, B., Hodell, D.A., Cutmore, A. & Eglinton, T.I. (2020) The impact of abrupt deglacial climate variability on productivity and upwelling on the southwestern Iberian margin. *Quaternary Science Reviews*, 230, 106139. Available from: https://doi.org/10.1016/j.quascirev.2019.106139

Bartolomé, M., Moreno, A., Sancho, C., Stoll, H.M., Cacho, I., Spötl, C., et al. (2015) Hydrological change in southern Europe responding to increasing North Atlantic overturning during Greenland Stadial 1. *Proceedings of the National Academy of Sciences*, 112(21), 6568–6572. Available from: https://doi.org/10.1073/pnas.1503990112

Bennett, K.D. & Willis, K.J. (2001) Pollen. In: Smol, J.P., Birks, H.J.B., Last, W.M., Bradley, R.S. & Alverson, K. (Eds.) *Tracking Environmental Change Using Lake Sediments: Terrestrial, Algal, and Siliceous Indicators, Developments in Paleoenvironmental Research*. Dordrecht: Springer, pp. 5–32. https://doi.org/10.1007/0-306-47668-1_2

Binford, M.W. (1990) Calculation and uncertainty analysis of ^{210}Pb dates for PIRLA project lake sediment cores. *Journal of Paleolimnology*, 3(3), 253–267. Available from: https://doi.org/10.1007/BF00219461

Blaauw, M. & Christen, J.A. (2011) Flexible paleoclimate age-depth models using an autoregressive gamma process. *Bayesian Analysis*, 6(3) 457–474. Available from: https://doi.org/10.1214/11-BA618

Blaauw, M., Christen, J.A., Bennett, K. & Reimer, P.J. (2018) Double the dates and go for Bayes: Impacts of model choice, dating density and quality on chronologies. *Quaternary Science Reviews*, 188, 58–66. Available from: https://doi.org/10.1016/j.quascirev.2018.03.032

Boavida, M.J. & Gliwicz, Z.M. (1996) Limnological and biological characteristics of the alpine lakes of Portugal. *Limnetica*, 12(2), 39–45. Available from: https://doi.org/10.23818/limn.12.11

Brauer, A. & Casanova, J. (2001) Chronology and depositional processes of the laminated sediment record from Lac d'Annecy, French Alps. *Journal of Paleolimnology*, 25, 163–177. Available from: https://doi.org/10.1023/A:1008136029735

Carrasco, R.M., Pedraza, J., Domínguez-Villar, D., Willenbring, J.K. & Villa, J. (2015) Sequence and chronology of the Cuerpo de Hombre paleoglacier (Iberian Central System) during the last glacial cycle. *Quaternary Science Reviews*, 129, 163–177. Available from: https://doi.org/10.1016/j.quascirev.2015.09.021

Connor, S.E., Araújo, J., van der Knaap, W.O. & van Leeuwen, J.F.N. (2012) A long-term perspective on biomass burning in the Serra da Estrela. *Quaternary Science Reviews*, 55, 114–124. Available from: https://doi.org/10.1016/j.quascirev.2012.08.007

Fisher, T.G. & Whitman, R.L. (1999) Deglacial and lake level fluctuation history recorded in cores, Beaver Lake, Upper Peninsula, Michigan. *Journal of Great Lakes Research*, 25(2), 263–274. Available from: https://doi.org/10.1016/S0380-1330(99)70735-5

Fletcher, W.J., Sánchez Goñi, M.F., Allen, J.R.M., Cheddadi, R., Combourieu-Nebout, N., Huntley, B., et al. (2010) Millennial-scale variability during the last glacial in vegetation records from Europe. *Quaternary Science Reviews*, 29(21–22), 2839–2864. Available from: https://doi.org/10.1016/j.quascirev.2009.11.015

García-Ruiz, J.M., Palacios, D., González-Sampériz, P., de Andrés, N., Moreno, A., Valero-Garcés, B., et al. (2016) Mountain glacier evolution in the Iberian Peninsula during the Younger Dryas. *Quaternary Science Reviews*, 138, 16–30. Available from: https://doi.org/10.1016/j.quascirev.2016.02.022

IPCC. (2022) In: Pörtner, H.-O., Roberts, D.C., Tignor, M., Poloczanska, E. S., Mintenbeck, K., Alegría, A., et al. (Eds.) *Climate Change 2022: Impacts, Adaptation and Vulnerability. Contribution of Working Group II to the Sixth Assessment Report of the Intergovernmental Panel on Climate Change*. Cambridge: Cambridge University Press.

Jambrina-Enríquez, M., Rico, M., Moreno, A., Leira, M., Bernárdez, P., Prego, R., et al. (2014) Timing of deglaciation and postglacial environmental dynamics in NW Iberia: The Sanabria Lake record. *Quaternary Science Reviews*, 94, 136–158. Available from: https://doi.org/10.1016/j.quascirev.2014.04.018

Lionello, P. (Ed). (2012) *The Climate of the Mediterranean Region: From the Past to the Future*. Amsterdam: Elsevier.

López-Sáez, J.A., Carrasco, R.M., Turu, V., Ruiz-Zapata, B., Gil-García, M.J., Luelmo-Lautenschlaeger, R., et al. (2020) Late Glacial–Early Holocene vegetation and environmental changes in the western Iberian central system inferred from a key site: The Navamuño record, Béjar range (Spain). *Quaternary Science Reviews*, 230, 106167. Available from: https://doi.org/10.1016/j.quascirev.2020.106167

Mayewski, P.A., Rohling, E.E., Stager, J.C., Karlén, W., Maasch, K.A., Meeker, L.D., et al. (2004) Holocene climate variability. *Quaternary Research*, 62(3), 243–255. Available from: https://doi.org/10.1016/j.yqres.2004.07.001

Migoń, P. & Vieira, G. (2014) Granite geomorphology and its geological controls, Serra da Estrela, Portugal. *Geomorphology*, 226, 1–14. Available from: https://doi.org/10.1016/j.geomorph.2014.07.027

Muñoz Sobrino, C., Heiri, O., Hazekamp, M., van der Velden, D., Kirilova, E.P., García-Moreiras, I., et al. (2013) New data on the Late Glacial period of SW Europe: A high resolution multiproxy record from Laguna de la Roya (NW Iberia). *Quaternary Science Reviews*, 80, 58–77. Available from: https://doi.org/10.1016/j.quascirev.2013.08.016

Naughton, F., Costas, S., Gomes, S.D., Desprat, S., Rodrigues, T., Sanchez Goñi, M.F., et al. (2019) Coupled ocean and atmospheric changes during Greenland Stadial 1 in southwestern Europe. *Quaternary Science Reviews*, 212, 108–120. Available from: https://doi.org/10.1016/j.quascirev.2019.03.033

Naughton, F., Sánchez Goñi, M.F., Kageyama, M., Bard, E., Duprat, J., Cortijo, E., et al. (2009) Wet to dry climatic trend in North-Western Iberia within Heinrich events. *Earth and Planetary Science Letters*, 284(3–4), 329–342. Available from: https://doi.org/10.1016/j.epsl.2009.05.001

Naughton, F., Sanchez Goñi, M.F., Landais, A., Rodrigues, T., Vazquez-Riveiros, N. & Toucanne, S. (2022) The Younger Dryas. In: Palacios, D., Hughes, P., García-Ruiz, J.M. & Andrés, N. (Eds.) *European Glacial Landscapes*. Amsterdam: Elsevier, pp. 51–57.

Naughton, F., Sanchez Goñi, M.F., Rodrigues, T., Salgueiro, E., Costas, S., Desprat, S., et al. (2016) Climate variability across the last deglaciation in NW Iberia and its margin. *Quaternary International*, 414, 9–22. Available from: https://doi.org/10.1016/j.quaint.2015.08.073

Oliva, M., Fernandes, M., Palacios, D., Fernández-Fernández, J.-M., Schimmelpfennig, I., Antoniades, D., et al. (2021) Rapid deglaciation during the Bølling–Allerød interstadial in the Central Pyrenees and associated glacial and periglacial landforms. *Geomorphology*, 385, 107735. Available from: https://doi.org/10.1016/j.geomorph.2021.107735

Oliva, M., Palacios, D., Fernández-Fernández, J.M., Rodríguez-Rodríguez, L., García-Ruiz, J.M., Andrés, N., et al. (2019) Late Quaternary glacial phases in the Iberian Peninsula. *Earth Science Reviews*, 192, 564–600. Available from: https://doi.org/10.1016/j.earscirev.2019.03.015

Palacios, D., Andrés, N., Marcos, J. & Vázquez-Selem, L. (2012) Maximum glacial advance and deglaciation of the Pinar Valley (Sierra de Gredos, Central Spain) and its significance in the Mediterranean context. *Geomorphology*, 177–178, 51–61. Available from: https://doi.org/10.1016/j.geomorph.2012.07.013

Rasmussen, S.O., Andersen, K.K., Svensson, A.M., Steffensen, J.P., Vinther, B.M., Clausen, H.B., et al. (2006) A new Greenland ice core chronology for the last glacial termination. *Journal of Geophysical Research: Atmospheres*, 111(D6), D06102. Available from: https://doi.org/10.1029/2005JD006079

Reimer, P., Austin, W.E.N., Bard, E., Bayliss, A., Blackwell, P.G., Bronk Ramsey, C., et al. (2020) The IntCal20 Northern Hemisphere radiocarbon age calibration curve (0–55 kcal BP). *Radiocarbon*, 62(4), 725–757. Available from: https://doi.org/10.1017/RDC.2020.41

Sánchez-López, G., Hernández, A., Pla-Rabes, S., Trigo, R.M., Toro, M., Granados, I., et al. (2016) Climate reconstruction for the last two millennia in Central Iberia: The role of East Atlantic (EA), North Atlantic Oscillation (NAO) and their interplay over the Iberian Peninsula. *Quaternary Science Reviews*, 149, 135–150. Available from: https://doi.org/10.1016/j.quascirev.2016.07.021

Scarlett, N.V.Y. & Madsen, I.C. (2006) Quantification of phases with partial or no known crystal structures. *Powder Diffraction*, 21(4), 278–284. Available from: https://doi.org/10.1154/1.2362855

Turu, V., Carrasco, R.M., López-Sáez, J.A., Pontevedra-Pombal, X., Pedraza, J., Luelmo-Lautenschlaeger, R., et al. (2021) Palaeoenvironmental changes in the Iberian central system during the late-glacial and Holocene as inferred from geochemical data: A case study of the Navamuño depression in western Spain. *Catena*, 207, 105689. Available from: https://doi.org/10.1016/j.catena.2021.105689

Turu, V., Carrasco, R.M., Pedraza, J., Ros, X., Ruiz-Zapata, B., Soriano-Lopez, J.M., et al. (2018) Late Glacial and post-Glacial deposits of the Navamuño peatbog (Iberian central system): Chronology and palaeoenvironmental implications. *Quaternary International*, 470, 82–95. Available from: https://doi.org/10.1016/j.quaint.2017.08.018

van der Knaap, W.O. & van Leeuwen, J.F.N. (1995) Holocene vegetation succession and degradation as responses to climatic change and human activity in the Serra de Estrela, Portugal. *Review of Palaeobotany and Palynology*, 89(3–4), 153–211. Available from: https://doi.org/10.1016/0034-6667(95)00048-0

van der Knaap, W.O. & van Leeuwen, J.F.N. (1997) Late Glacial and Early Holocene vegetation succession, altitudinal vegetation zonation, and climatic change in the Serra da Estrela, Portugal. *Review of Palaeobotany and Palynology*, 97(3–4), 239–285. Available from: https://doi.org/10.1016/S0034-6667(97)00008-0

Vieira, G. (2008) Combined numerical and geomorphological reconstruction of the Serra da Estrela plateau icefield, Portugal. *Geomorphology*, 97(1–2), 190–207. Available from: https://doi.org/10.1016/j.geomorph.2007.02.042

Vieira, G., Palacios, D., Andrés, N., Mora, C., Vázquez Selem, L., Woronko, B., et al. (2021) Penultimate glacial cycle glacier extent in the Iberian Peninsula: New evidence from the Serra da Estrela (central system, Portugal). *Geomorphology*, 388, 107781. Available from: https://doi.org/10.1016/j.geomorph.2021.107781

Vieira, G. & Woronko, B. (2022) Chapter 4.16 - The glaciers of Serra da Estrela. In: Oliva, M., Palacios, D. & Fernández-Fernández, J.M. (Eds.) *Iberia, Land of Glaciers*. Amsterdam: Elsevier, pp. 417–435. https://doi.org/10.1016/B978-0-12-821941-6.00020-7

Wei, D., González-Sampériz, P., Gil-Romera, G., Harrison, S.P. & Prentice, I.C. (2021) Seasonal temperature and moisture changes in interior semi-arid Spain from the last interglacial to the Late Holocene. *Quaternary Research*, 101, 143–155. Available from: https://doi.org/10.1017/qua.2020.108

Wilson, R., Glasser, N.F., Reynolds, J.M., Harrison, S., Anacona, P.I., Schaefer, M., et al. (2018) Glacial lakes of the central and Patagonian Andes. *Global and Planetary Change*, 162, 275–291. Available from: https://doi.org/10.1016/j.gloplacha.2018.01.004

Yu, Z. & Eicher, U. (2001) Three amphi-Atlantic century-scale cold events during the Bølling–Allerød warm period. *Géographie Physique et Quaternaire*, 55(2), 171–179. Available from: https://doi.org/10.7202/008301ar

SUPPORTING INFORMATION

Additional supporting information can be found online in the Supporting Information section at the end of this article.